Twisted ABC Triblock Copolymer Cylinders with Segregated A and C Coronal Chains

Jiwen Hu, Gabriel Njikang, and Guojun Liu*

Department of Chemistry, Queen's University, 90 Bader Lane, Kingston, Ontario, Canada K7L 3N

Received July 18, 2008; Revised Manuscript Received September 5, 2008

ABSTRACT: The formation of twisted cylinders with segregated A and C coronal chains from an ABC triblock copolymer in a block-selective solvent for the A and C blocks is reported. Such cylinders consisted of left- and right-handed helical sections (3D twisting) connected by wriggling (2D twisting) sections after aspiration on a solid substrate. The copolymer used was poly(glyceryl monomethacrylate)-*block*-poly(2-cinnamoyloxyethyl methacrylate)-*block*-poly(*tert*-butyl acrylate) or PGMA-*b*-PCEMA-*b*-PtBA consisting of 310 PGMA units, 130 CEMA units, and 110 tBA units. Twisted cylinders were prepared from the dialysis of an aqueous solution of the triblock copolymer against methanol. In water, the copolymer formed core−shell−corona cylinders with the insoluble PtBA and PCEMA blocks making up the core and shell and the soluble PGMA block making up the corona. The cylinders with PCEMA cores twisted in water/methanol with high methanol contents, e.g., >90 vol%, probably to create more space to accommodate the segregated PGMA chains, which were longer, better solvated, and more crowded than the PtBA chains. Also investigated is the mechanism for the morphological transition from the core−shell−corona cylinders in water to the twisted cylinders in water/methanol.

I. Introduction

The association of block copolymers in block-selective solvents yields micelle-like aggregates (MAs) with shapes ranging from spheres[1] to vesicles,[2–5] nanotubes,[6] linear cylinders,[7,8] branched cylinders,[9] looped cylinders,[3,10,11] and segmented cylinders etc.[12,13] The shape diversity of such aggregates facilitates their applications in nanofabrication,[14–16] lithography,[17–19] cell culturing,[20,21] and drug delivery.[22,23] Most past morphological studies of MAs were performed for diblock copolymers.[1] When ABC linear triblock copolymers were studied, solvents selective for one terminal block (A or C) or two consecutive blocks (A and B or B and C) were typically used.[24] With rare exceptions for ABC linear triblock copolymers[25,26] and exceptions for ABC mikto-star triblock copolymers,[27,28] the use of such solvents led to the formation core−shell−corona spheres[29–33] or core−shell−corona cylinders.[14,34–36] We report in this paper the preparation of MAs from an ABC triblock copolymer in a block-selective solvent for the A and C blocks and the discovery of a novel MA morphology, which consists of twisted B cylinders covered by segregated A and C coronal chains. Such cylinders contain both left- and right-handed helical (3D twisting) sections connected by wriggling (2D twisting) sections after aspiration on a solid substrate.

Specifically, the triblock copolymer used in this study was poly(glyceryl monomethacrylate)-*block*-poly(2-cinnamoyloxyethyl methacrylate)-*block*-poly(*tert*-butyl acrylate) or PGMA-*b*-PCEMA-*b*-PtBA.

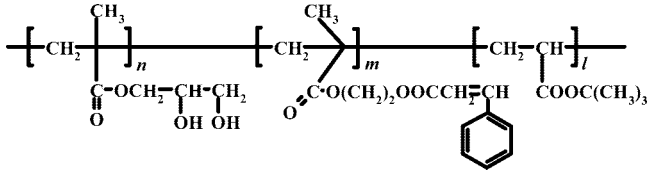

This polymer was targeted because methanol could be used as a block-selective solvent for the PGMA and PtBA blocks. With PGMA being hydrophilic and PtBA hydrophobic, we suspected that the two terminal blocks should be highly incompatible and segregate in the corona of the MAs formed. PCEMA was used because it could be photocrosslinked to lock in the structure of the MAs[34,37,38] to facilitate their structural elucidation.

Single-handed helical cylinders with many pitches have been prepared from the self-assembly in block-selective solvents of diblock copolymers containing a chiral block.[39,40] These helical cylinders twisted single-handedly for the chirality and thus the oriented packing of the chiral block. Recently, Pochan, Wooley, and co-workers[25] reported formation of helical cylinders from a triblock copolymer, poly(acrylic acid)-*block*-poly(methyl methacrylate)-*block*-polystyrene or PAA-*b*-PMMA-*b*-PS, in water/tetrahydrofuran (THF) containing triethylenetetramine or other multiamines. Here, the water/THF mixture was selective for PAA. For lack of chiral centers, the cylinders were not single-handed. The PS-PMMA core−shell cylinders twisted presumably for the uniaxial compression of the cylinders along the cylinder axis, and the compression forces were thought to arise from complex formation between the multiamines and PAA. Aside from being in block-selective solvents, the helical morphology has been observed also in block copolymer solids. For example, Krappe et al.[41] discovered the formation of helical cylinders from the B block in an ABC triblock copolymer solid. Helical cylinders have been observed also for the A block of an AB diblock copolymer that had undergone self-assembly in the confinement of the tubular pores of an anodized alumina membrane.[42]

The cylindrical PCEMA core of the PGMA-*b*-PCEMA-*b*-PtBA MAs twisted in water/methanol with high methanol contents, e.g., >90 vol%, probably to create more space for the segregated PGMA chains, which were longer, better solvated, and more crowded than the PtBA chains. Our twisted cylinders (TCs) were formed for a mechanism that was different from those that have been reported. They were unique in structure for the segregation of their coronal chains. While the segregation of different polymers in the solid state[43] or in concentrated polymer solutions[44] is well-known, the observation of segregation of solvated coronal chains on the surfaces of MAs or polymer nanoparticles has rarely been observed.[45–47]

* To whom correspondence should be addressed. E-mail: guojun.liu@chem.queensu.ca.

10.1021/ma801626y CCC: $40.75
Published on Web 10/14/2008

II. Experimental Section

Materials. Methanol (99.8+%), methylene chloride (99.5+%), and hydrochloric acid (36.5−38.0 wt%) were purchased from Fisher Scientific and were used as received. Inhibitor-free tetrahydrofuran (THF) from Fisher Scientific was dried by filtration through a system equipped with two alumina columns from Innovative Technology, Inc. Diethyl ether (class-1A, Fisher Scientific) was distilled before use. Pyridine (Aldrich, 99+%) was refluxed with calcium hydride (Aldrich, regent grade, 95%) overnight and distilled prior to use. The staining agents osmium oxide OsO_4 and uranyl acetate $UO_2(Ac)_2 \cdot H_2O$ were purchased from Electron Microscopy Sciences and were used without further purification. Trifluoroacetic acid (99+%), cinnamoyl chloride (98%, predominantly *trans*), and *N*, *N*-dimethylformamide (DMF) were all purchased from Aldrich and were used as received. The staining agent RuO_4 was prepared from reacting ruthenium chloride hydrate (Aldrich) and sodium hypochlorite (Aldrich, 10−13% chlorine) in water just before use.[48] The dialysis tubes used were purchased from Spectrum Laboratories, Inc. They had a molecular-weight cutoff of 12 000−14 000. Silicon wafers with orientation (100) were purchased from Silicon Quest International.

PSMA-*b*-PCEMA-*b*-PtBA. PSMA-*b*-PCEMA-*b*-PtBA was prepared by reacting PSMA-*b*-PHEMA-*b*-PtBA with cinnamoyl chloride. Here, PSMA and PHEMA denote poly(solketal methacrylate) and poly(2-hydroxyethyl methacrylate), respectively. Since the preparation of PSMA-*b*-PCEMA-*b*-PtBA of a different composition has been described before,[15,49] the procedure is not repeated here.

PGMA-*b*-PCEMA-*b*-PtBA. PSMA-*b*-PCEMA-*b*-PtBA, 0.10 g, was stirred for 20 min in 4 mL of THF before 1.0 mL of 6.0-M HCl was added dropwise under stirring. The addition of the HCl solution decreased the triblock copolymer solubility and turned the resultant mixture cloudy. The solution turned clearer 0.5 h after HCl addition for PSMA hydrolysis. Despite this, the hydrolysis reaction was allowed to proceed for another 3 h before the final mixture was dialyzed against methanol to remove small-molecule impurities. The methanol was changed 8× over 48 h.

Cylindrical Micelle-like Aggregates in Water. The above PGMA-*b*-PCEMA-*b*-PtBA solution, ∼20 mL, was added into 200 mL of diethyl ether. The resultant suspension was centrifuged at 2880 rpm (1550 ×*g*) for 5 min to settle the polymer. After ether decantation, 15 mL of water was added to 45 mg of PGMA-*b*-PCEMA-*b*-PtBA under magnetic stirring at 1000 rpm. The mixture was stirred at room temperature for 3−5 d to yield mostly cylindrical micelle-like aggregates or CMAs in water, which solubilized only the PGMA block.

Twisted Cylinders. The aqueous CMA solution above was dialyzed against methanol changed 8× over 48 h. This yielded TCs in water/methanol with essentially pure methanol or methanol at ∼3 mg/mL. Unless otherwise mentioned, TCs in methanol in the rest of this paper will refer to samples prepared from this standard method.

We also tested if TCs could be prepared by directly dispersing in methanol PGMA-*b*-PCEMA-*b*-PtBA freshly precipitated from diethyl ether. For this, a PGMA-*b*-PCEMA-*b*-PtBA solution in methanol, 2.5 mL at ∼6 mg/mL, was added into 7.5 mL of diethyl ether. The mixture was centrifuged at 2880 rpm (1550 g) for 5 min to settle the polymer. After removing the supernatant, 5 mL of methanol was added to the precipitate under magnetic stirring at 1000 rpm. The mixture was left stirring for 1 week before aspiration and sample staining by OsO_4 for TEM analysis. TEM analysis indicated that wriggly cylinders with occasional helical sections were obtained.

Micelle-like Aggregate Cross-Linking. TCs at 3.0 mg/mL in 3.0 mL of methanol were irradiated by a focused beam that had passed through a 270 nm cutoff filter for 4 h under magnetic stirring. The photolysis system consisted of a 500-W mercury lamp in an Oriel 6140 lamp housing. The lamp was powered by an Oriel 6128 power supply. PCEAM double bond conversion was estimated from absorbance decrease at 274 nm to be 34%.[37]

Hydrolysis of PtBA to PAA. Cross-linked TCs in methanol were bubbled with N_2 to remove most of the solvent before being dried under vacuum at room temperature overnight. The TCs were redispersed in 3.0 mL of methylene chloride. To the solution under stirring was added dropwise 1.0 mL of trifluoroacetic acid. The mixture was left stirring for 4 h at room temperature before 10 mL of methanol was added. The dispersion was bubbled with N_2 to remove most of the volatile solvent before 3 mL of DMF was added slowly. The resultant dispersion was dialyzed against DMF by changing DMF 3 times over 24 h to remove small molecule impurities.

Morphological Transition from CMAs to TCs. Freshly precipitated PGMA-*b*-PCEMA-*b*-PtBA, 12.0 mg, was stirred with 1.0 mL of water for 5 d. To the resultant CMAs was added under stirring over 9 min 9.0 mL of methanol. This solution was stirred for another 5 min before an aliquot was taken and aspirated immediately on a nitrocellulose-coated copper grid for later TEM analysis. This sample was denoted as transition state sample 1 or TS1.

Within 1 to 2 min or immediately after the aspiration of TS1, the rest of the copolymer in water/methanol at $v/v = 1/9$ was transferred into a dialysis tube. The tube was then immersed in 90 mL of fresh methanol. After 15 min, another aliquot was taken and aspirated immediately for later TEM analysis. This sample was denoted as TS2.

TS3 was obtained after the residual copolymer solution was equilibrated with another 90 mL of fresh methanol for 15 min. This procedure was repeated another 2× to yield TS4 and TS5. The residual sample after TS5 removal was dialyzed against 90 mL of fresh methanol for 30 min to yield TS6. TS7 was obtained after dialyzing the residual copolymer solution against another 90 mL of fresh methanol for 60 min.

The above process yielded samples for staining by OsO_4. A TS2 sample with PtBA hydrolyzed and the resultant PAA stained was prepared as follows. To 1.0 mL of a CMA solution in water at 10 mg/mL was added 9.0 mL of methanol over 9 min. The solution was stirred for 5 min and then dialyzed against 90 mL of methanol for 15 min. The sample was subsequently treated to cross-link PCEMA and hydrolyze PtBA following procedures described above.

Transmission Electron Microscopy Measurements. Aggregates in methanol, water, or water/methanol were aspirated onto nitrocellulose- or carbon-coated copper grids. After drying under vacuum at room temperature for 2 h, the samples were stained by either OsO_4 vapor for 2 h or RuO_4 vapor for 1 h before observation by transmission electron microscopy (TEM). The DMF solutions of TCs or TS2 with PtBA hydrolyzed were aspirated onto a 3 × 3 mm^2 mica-supported carbon film. After DMF evaporation under vacuum at room temperature, one drop of a uranyl acetate solution in DMF at 0.05 g/mL was added onto the film to stain the AA groups for 30 min. The excess staining agent was sucked off with a filter paper. The sample was rinsed with 2 mL of methanol/water at $v/v = 4/1$ before the carbon film was floated off the mica plate on to the surface of deionized water. The carbon film was picked up by a TEM copper grid and evacuated to remove water before TEM observation. All TEM images were obtained on a Hitachi-7000 instrument operated at 75 kV.

Atomic Force Microscopy Observations. Specimens were prepared by aspirating solution samples onto silicon wafers. All samples were analyzed by tapping-mode atomic force microscopy (AFM) using a Veeco multimode instrument equipped with a Nanoscope IIIa controller. The tips used were of the Nanosensors NCHR-SPL type with a tip radius of ∼5 nm. The images were obtained using a free tip oscillation amplitude A_0 of 60 nm and a set point amplitude ratio R_{sp} of ∼90%.

PtBA Solubility Test. PtBA used for solubility test was prepared by anionic polymerization using a monomer to initiator molar feed ratio of 100. On the basis of polystyrene standards, the size-exclusion molecular weight characteristics of the sample were $M_w = 1.4 \times 10^4$ g/mol and $M_w/M_n = 1.09$. For solubility test, 10.0 mg of PtBA was dissolved in 3.6 mL of methanol in a 6 mL vial capped

Table 1. Molecular Properties of PSMA-*b*-PCEMA-*b*-PtBA

SEC M_w/M_n	dn_r/dc (mL/g)	LS $10^{-5}M_w$	NMR *n/m/l*	n_w	m_w	l_w
1.17	0.141	1.1	1.00/0.43/0.36	310	130	110

with a rubber septum. Water was then injected dropwise under shaking till the solution turned cloudy. This required a total of 275 μL or 7 vol% of deionized water.[50]

III. Results and Discussion

Triblock Copolymer Characterization. The PGMA-*b*-PCEMA-*b*-PtBA sample was characterized in the PSMA-*b*-PCEMA-*b*-PtBA form for the similar solubility in common organic solvents of the three blocks of PSMA-*b*-PCEMA-*b*-PtBA. The detailed procedure for the characterization of such samples have been reported before[35,51] and was thus not repeated in the Experimental Section. The repeat unit number ratios *n/m/l* were determined from comparing the ^{1}H NMR peaks of the three blocks of the copolymer. The specific refractive index increment dn_r/dc and the light scattering (LS) molecular weight M_w of the copolymer were determined in butanone. The polydispersity index M_w/M_n of the sample was measured by size-exclusion chromatography (SEC) in THF based on polystyrene standards. By combining the *n/m/l* and light scattering M_w values, the weight-average repeat unit numbers n_w, m_w, and l_w for the PSMA, PCEMA, and PtBA blocks were calculated to be 310, 130, and 110, respectively (Table 1).

Micelle-like Aggregates in Water. Figure 1a, c shows TEM images and part b shows an AFM topography image of the MAs aspirated from water. Here, the TEM specimens were stained by the PCEMA-selective OsO_4. The figure suggests that most of the aggregates were cylinders. The cylinders could be straight, bent, branched, or looped. Coexisting with the cylinders were some spherical aggregates. The weight fraction of the spherical aggregates was low. For this, our following discussion will focus on the cylindrical aggregates only.

Many of the linear cylinders had spherical end caps with diameters substantially larger than those of their main part. Even the main part of some cylinders was not smooth but bore bumps and abnormally fat sections containing dark inner PCEMA domains (Figure 1c). These features appear to have resulted from the incomplete integration of spherical aggregates into the cylinders. Our suspicion is that at least some of the cylinders were formed from the fusion of spherical aggregates. The spherical aggregates did not fully incorporate into the cylinders at room temperature probably because of the high glass transition temperatures of 69 and 73 °C for PCEMA[52] and PtBA.[49,53] Since the focus of this study was not on these cylinders but on TCs formed in methanol or water/methanol, we did not pursue this issue further.

We measured the diameters of >300 sections of 50 CMAs that did not contain bumps or abnormally fat sections from different TEM images and yielded an average TEM diameter of 36 ± 4 nm. We unfortunately could not determine the internal structure of the CMAs from Figure 1a, c. Such CMAs should have a PGMA corona because this was the only water-soluble block in the copolymer. To demonstrate that they had a PtBA core, we photolyzed the aggregates in water with UV light to cross-link the PCEMA shell.[37] The PtBA cores in such "permanent" structures were then hydrolyzed to yield poly(acrylic acid)- or PAA-lined tubular cores.[54] After aspirating the nanotubes on a nitrocellulose-coated copper grid and staining the PAA groups with uranyl acetate, we obtained TEM images with one shown in Figure 1d. The occurrence of an uneven dark "ribbon" in the center of each elongated object confirms unambiguously that a tubular structure existed. The "ribbon" width varied among different sections of the same tube, because the tube collapsed to different degrees in different sections.

Averaging over ~50 readings, the height and diameter for the smooth parts of the CMAs were determined from the AFM image of Figure 1b to be 41 ± 4 and 79 ± 6 nm, respectively. The true diameter of the CMAs should be between the AFM height and diameter values for CMA flattening on a substrate. Aside from flattening, the AFM diameter also contained a tip thickness contribution. The fact that the TEM diameter is less than the AFM height of 41 ± 4 nm suggests that PGMA was probably not seen by TEM but detected by AFM.

Twisted Cylinders. TCs were prepared by dialyzing the CMA solutions in water against methanol. Figure 2a, b shows TEM images of aspirated TCs stained by OsO_4 and RuO_4, respectively. Two AFM topography images of the TCs on silicon are shown as Figure 2c, d.

Figure 2a shows that the cylinders can be doughnut-like when they are short. The long ones typically contain both helical (3D twisting) and wriggling (2D winding) sections. The helical sections can be either right-handed, as those marked by the cyan arrows, or left-handed, as marked by the white arrows in Figure 2, parts a, b, and d. The pitch length of the helical sections varied greatly from one to another and was typically less than 200 nm. The cylinders in Figure 2a have an average diameter of 14.7 ± 2.1 nm. The cylinders in Figure 2b appear substantially thicker and have a diameter of 27.4 ± 2.1 nm. The difference must have resulted from the staining of not only PCEMA but also PGMA by RuO_4 and of only PCEMA by OsO_4.

A fully stretched PCEMA chain with 135 units has an end-to-end distance of 34 nm. In the unperturbed state, such a chain has a root-mean-square end-to-end distance of 8.2 nm, if its statistical bond length is assumed to be 0.5 nm.[55] Thus, the PCEMA diameter value of 14.7 ± 2.1 nm from Figure 2a suggests some stretching of the PCEMA core chains from its unperturbed state, a phenomenon that is common to many micellar systems.[8,56–58]

TCs were observed regardless of whether carbon, nitrocellulose, mica, or silicon was used as the support for TEM and AFM specimen preparation. This suggests that the TCs could not have formed due to a specific polymer/substrate interaction. Furthermore, the TCs were seen in essentially equal amounts regardless if the PCEMA cores of the samples were photocrosslinked. PCEMA cross-linking was supposed to lock in and rigidify[37,59] the aggregates formed in methanol and to drastically reduce PCEMA chain mobility. The fact that TCs were observed in the cross-linked samples suggests their presence in methanol already. The fact that TCs were seen also in noncross-linked samples suggests insignificant morphological mutations for the uncrosslinked aggregates during TEM or AFM specimen preparation.

To probe the distribution of the coronal PtBA and PGMA chains, we photocrosslinked the PCEMA core of the TCs in methanol. The PtBA coronal chains were then hydrolyzed to PAA chains. The resultant cylinders bearing PAA chains were aspirated from DMF on carbon-coated copper grids and stained by uranyl acetate for TEM study. Figure 3 shows a TEM image of such a sample. The cylinder here does not appear helical but wriggly. The diameter of the gray cylinder is 27.9 ± 3.2 nm, which is comparable to 27.4 ± 2.1 nm found for the cylinders in Figure 2b. Embedded in the gray cylinder are segmented dark PAA threads and PAA dots. The PAA threads have a diameter of 7.3 ± 1.1 nm and oscillate from one side of the gray cylinder to another. They sit preferentially on the concave side of the cylinder. In the straight sections marked by arrows, distinct PAA threads are missing.

The cylinder of Figure 3 does not appear helical probably for the multiple chemical treatment and solvent switching steps that it had gone through. Also, it was aspirated from DMF rather

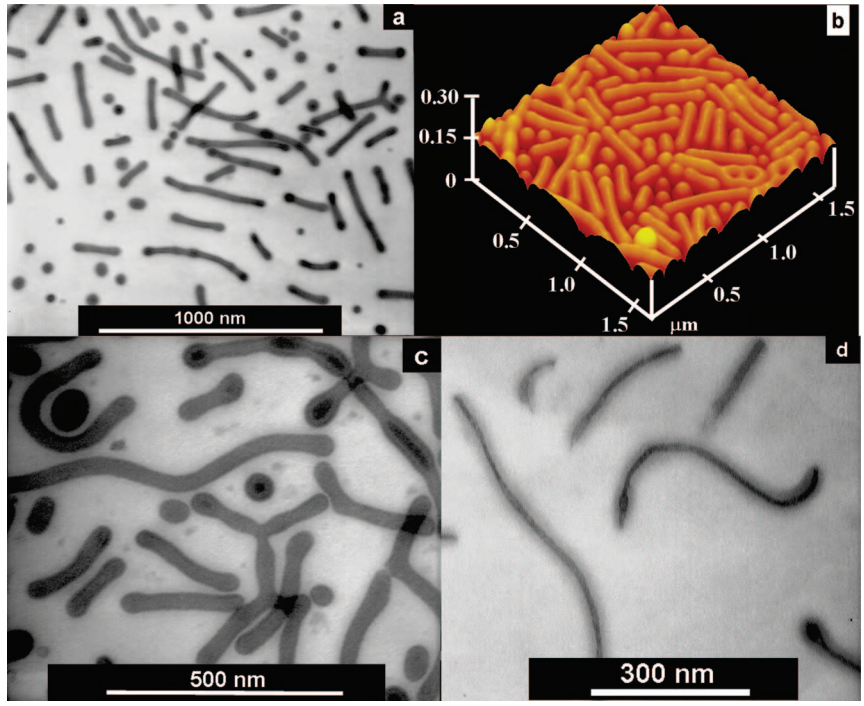

Figure 1. TEM (a and c) and AFM topography (b) images of MAs aspirated from water. Also shown is a TEM image (d) of the MAs after PCEMA shell cross-linking and PtBA hydrolysis. The last specimen was stained by uranyl acetate.

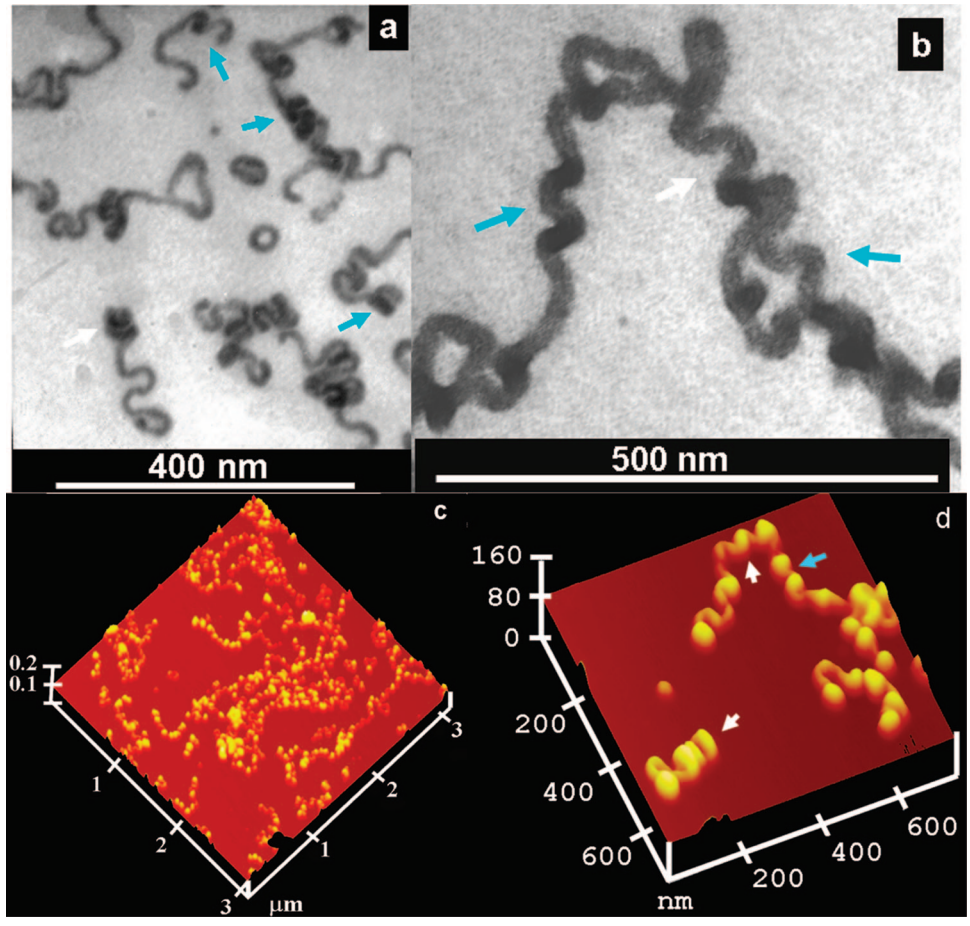

Figure 2. TEM (a and b) and AFM topography (c and d) images of PGMA-*b*-PCEMA-*b*-PtBA helical nanocylinders. For TEM imaging, the specimens were stained by OsO_4 (a) and RuO_4 (b), respectively.

than from methanol. Unlike methanol, DMF was not a block-selective solvent and should swell the cross-linked PCEMA block. Thus, the conformation of the cylinder in DMF might have been different from that in methanol.

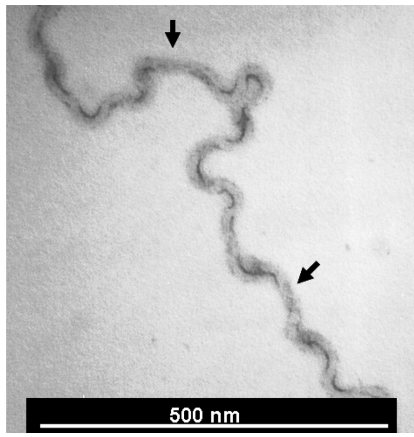

Figure 3. TEM image of a helical cylinder aspirated from DMF. The PCEMA block of the sample was photocrosslinked, the PtBA block was hydrolyzed, and the resultant PAA chains were stained by uranyl acetate.

Figure 4. Schematic of the chain packing in the CMAs and TCs. The cyan, red, and black colors denote the PGMA, PCEMA, and PtBA domains, respectively.

Observation of distinct PAA dots and threads in the gray cylinder of Figure 3 suggests segregation of the original PtBA chains from the PGMA chains. It occurred cleanly here probably mainly for the high incompatibility between PtBA and PGMA. The coronal chain segregation was enhanced probably also by the way how the TCs were prepared as will be discussed later. The high incompatibility can be appreciated from a chemical structural comparison of the two. With PGMA being water soluble, we suspect that PtBA should be much less polar than the PGMA. We have also performed an empirical calculation of the solubility parameters δ of the polymers. Such an empirical calculation[60] yielded very different δ values of 18.6 and 28.7 $MPa^{1/2}$ for PtBA and PGMA, respectively.

Figure 4 depicts schematically our current understanding of the structures of the CMAs and TCs. Only one helical section rather than multiple helical and wriggly sections of a TC were drawn for convenience. Aside from this, the PtBA and PGMA chain distribution patterns depicted should be treated as being approximate. Furthermore, the sizes of the different domains were not to scale.

Transition from Core−Shell−Corona to Twisted Cylinders. To know how the TCs were formed, we performed controlled solvent switching from water to methanol and took samples at different stages for TEM analyses. Figure 5a−d shows TEM images for some of these samples. Figures 5a is a TEM image for transition state sample 1 or TS1. It was taken and aspirated for TEM analysis after the addition of 9.0 mL of methanol over 9 min into 1.0 mL of a CMA solution in water and the stirring of the resultant mixture for 5 min. TS2 of Figure 5b was obtained after the residual mixture from TS1 was dialyzed against 90 mL of methanol for 15 min. The specimens for these images were stained by the PCEMA-selective OsO_4. To obtain the image of Figure 5c, a sample that was prepared analogously as TS2 was irradiated with UV light to cross-link PCEMA and treated with trifluoroacetic acid to hydrolyze PtBA. The resultant sample was then aspirated and stained by $UO_2(Ac)_2$. TS3 of Figure 5d was obtained after the residual mixture from TS2 was dialyzed against another 90 mL of methanol for 15 min. Such further solvent changing and dialysis experiment was continued as described in the Experimental Section until TS7 was obtained.

The TEM images of the original sample aspirated from water and stained by OsO_4 should be similar to those shown in Figure

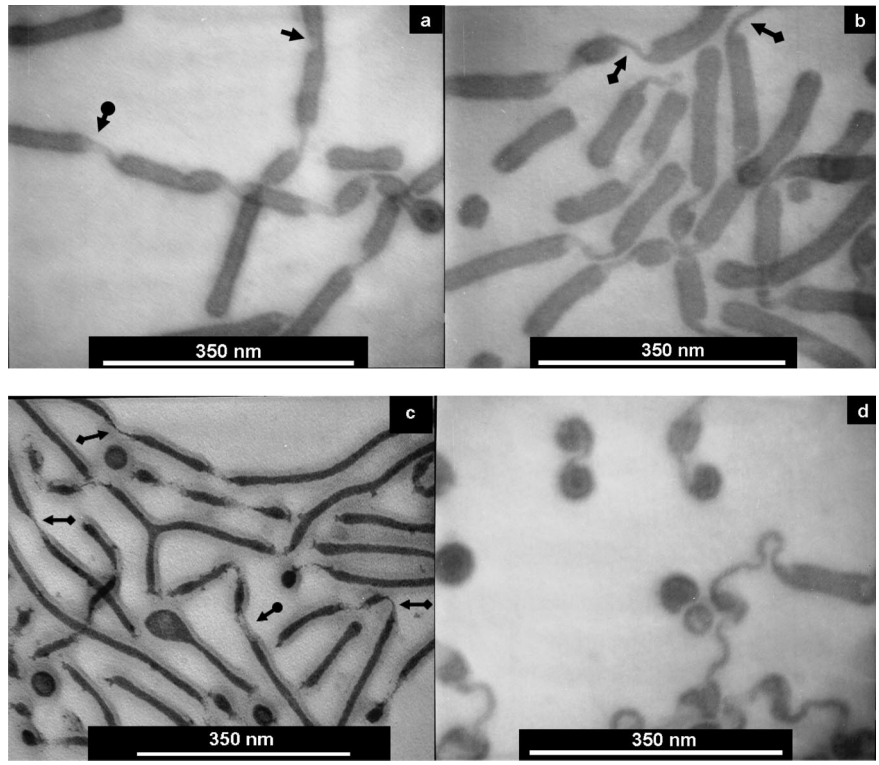

Figure 5. TEM images of TS1 (a), TS2 (b and c), and TS3 (d) aspirated on copper grids coated by nitrocellulose. The specimens for images a, b, and d were stained by OsO_4. The sample for image c was photolyzed to cross-link PCEMA and treated by CF_3COOH to hydrolyze PtBA. The resultant PAA chains were stained by $UO_2(Ac)_2$ after sample aspiration.

1a, c. After the introduction of methanol to a final volume fraction of 90% for TS1, dents or fractures (one marked by a regular arrow in Figure 5a) appeared on certain sections of the CMAs. Also, the cylinders had broken into sections connected by ribbons (one marked by an arrow with a circular end in Figure 5a) and thin threads or rods (some marked by arrows with square end in Figure 5b). The threads were longer in Figure 5, part b than in part a and were the longest in part d. By TS6, all of the CMA sections disappeared and only TCs were observed.

Ribbons and threads were seen also in Figure 5c, where the specimen was stained by $UO_2(Ac)_2$. Here, the PAA domains were clearly seen with the PCEMA and PGMA parts visible sometime as shadows around the PAA domains. The structure marked by an arrow with a circular end was most likely a ribbon. Those marked by arrows with square ends were probably structures with their middle parts already transformed into threads.

The TEM images of Figure 5 and those for TS4−TS7 (not shown) suggest the following mechanism for the formation of the twisted cylinders. First, dents were formed or the PCEMA shell ruptured at certain and probably defective spots of the CMAs. Then, the dents grew or the tip of the cracks propagated along the CMA axial direction to generate PCEMA ribbons covered on their opposite sides by PtBA and PGMA. Concurrently, the ribbons shrank laterally and elongated longitudinally to generate twisted PCEMA threads or rods covered by PtBA and PGMA.

The PCEMA shells ruptured most likely from the swelling of the PtBA core chains by methanol or water/methanol. We have determined that water/methanol with >93 vol% methanol solubilized a PtBA homopolymer with ~100 repeat units. The PtBA block of the PGMA-*b*-PCEMA-*b*-PtBA sample should have a similar solubility and should swell substantially even at a methanol content of 90 vol% when TS1 was taken.

The tip of the dents or cracks propagated along the CMA axial direction probably for the propagation also along the same direction of a methanol flux, which entered the PtBA core from the dents. The PCEMA ribbons shrank laterally, probably mainly to decrease the PCEMA/solvent interfacial area and also to eliminate the ribbon edges, which were not covered by PGMA or PtBA chains and should have a higher surface energy than the central part of a ribbon. In water/methanol with <93 vol% methanol and when the PtBA chains were not soluble yet, the tendency for the PtBA chains to cluster may have helped provide another driving force for the ribbon lateral shrinkage. This lateral contraction was unfortunately accompanied by an increase in the crowding of the surface PGMA chains. The need to reduce the PGMA chain repulsion drove the PCEMA layer to stretch along the cylinder axial or longitudinal direction. In the end, the PCEMA domain got rid of the edges by changing from a ribbon into a cylindrical thread with the surface chains not shuffled or remaining segregated.

The TEM results of Figure 5 suggest that the PCEMA domains twisted when the PCEMA ribbons shrank into threads. The TEM image of Figure 3 showed that the PtBA chains segregated from the PGMA chains and occurred mostly on the concave side or the interior of a helical section (Figure 4). On the exterior of a helical section, the PGMA chains should have more space to accommodate themselves and should thus have an interchain repulsion weaker than what would be found if the PCEMA core cylinder remained straight. Thus, our hypothesis was that the PCEMA cylinder twisted to eliminate a net lateral force generated by the longer and more strongly repelling PGMA chains. Aside from chain length asymmetry, the lower solubility of the PtBA chains than the PGMA chains in water/MeOH probably also helped magnify the surface lateral force imbalance.

While the mechanism of twisted cylinder formation resulting from a surface lateral force imbalance is new for block copolymers, it has been observed in many small molecule systems. For example, mixed bilayers can be prepared in water containing Ca^{2+} from a mixture of an acidic phospholipid and phosphatidylcholines. Here, the phospholipid has a negatively charged phosphate head and the phosphatidylcholines has a zwitterion head. When prepared in water containing Ca^{2+}, the two types of surfactants in the formed bilayers phase-separated laterally because of selective binding of Ca^{2+} with the acidic phospholipid. Lin et al.[61] found that such phase-separated bilayers with nonuniform lateral forces or tensions folded into single- and double-helical liposomes under appropriate conditions. Huang[62] has proposed a general theory for the coiling of phospholipid tubes, which consist of many concentric tubular bilayers of phospholipids. Tube twisting was again assumed to be triggered by a lateral tension asymmetry.

IV. Conclusions

A PGMA-*b*-PCEMA-*b*-PtBA triblock copolymer self-assembled in water into core−shell−corona cylindrical aggregates. After the aqueous solution was dialyzed against methanol, the CMAs were transformed into twisted cylinders. TEM and AFM were used to establish the structures of the CMAs, TCs, and the intermediates for the transition. TEM evidence suggests that the addition of methanol into the CMA solution caused the PCEMA shell to rupture at spots. After rupturing, the newly formed PCEMA ribbons started to contract laterally, stretch longitudinally, and eventually evolved into twisted PCEMA thin cylinders. The TCs grew at the expense of the old CMAs. Our TEM results suggest that the surface PtBA and PGMA chains were highly incompatible and segregated. The cylinders twisted probably for a surface lateral force imbalance between the PGMA and PtBA chains with much different lengths. The generality of this mechanism for producing twisted cylinders remains to be discovered.

Acknowledgment. NSERC of Canada is thanked for sponsoring this research. The Outstanding Overseas Chinese Scholar Funds of the Chinese Academy of Sciences is thanked for covering J.W.H.'s travel expenses. J. D. Wang is thanked for obtaining AFM images. G.L. thanks the Canada Research Chairs program for a research chair position in Materials Science.

References and Notes

(1) Lazzari, M.; Liu, G. J.; Lecommandoux, S. *Block Copolymers in Nanoscience*; Wiley-VCH: Weinheim, Germany, 2006.
(2) Zhang, L. F.; Eisenberg, A. *Science* **1995**, *268*, 1728–1731.
(3) Ding, J. F.; Liu, G. J.; Yang, M. L. *Polymer* **1997**, *38*, 5497–5501.
(4) Ding, J. F.; Liu, G. J. *Macromolecules* **1997**, *30*, 655–657.
(5) Discher, D. E.; Eisenberg, A. *Science* **2002**, *297*, 967–973.
(6) Raez, J.; Manners, I.; Winnik, M. A. *J. Am. Chem. Soc.* **2002**, *124*, 10381–10395.
(7) Price, C. *Pure Appl. Chem.* **1983**, *55*, 1563–1572.
(8) Tao, J.; Stewart, S.; Liu, G. J.; Yang, M. L. *Macromolecules* **1997**, *30*, 2738–2745.
(9) Jain, S.; Bates, F. S. *Science* **2003**, *300*, 460–464.
(10) Chen, Z. Y.; Cui, H. G.; Hales, K.; Li, Z. B.; Qi, K.; Pochan, D. J.; Wooley, K. L. *J. Am. Chem. Soc.* **2005**, *127*, 8592–8593.
(11) Zhu, J. T.; Liao, Y. G.; Jiang, W. *Langmuir* **2004**, *20*, 3809 3812.
(12) Cui, H. G.; Chen, Z. Y.; Zhong, S.; Wooley, K. L.; Pochan, D. J. *Science* **2007**, *317*, 647–650.
(13) Li, Z. B.; Kesselman, E.; Talmon, Y.; Hillmyer, M. A.; Lodge, T. P. *Science* **2004**, *306*, 98–101.
(14) Liu, G.; Yan, X.; Li, Z.; Zhou, J.; Duncan, S. *J. Am. Chem. Soc.* **2003**, *125*, 14039–14045.
(15) Yan, X.; Liu, G.; Li, Z. *J. Am. Chem. Soc.* **2004**, *126*, 10059-10066.

(16) Massey, J. A.; Winnik, M. A.; Manners, I.; Chan, V. Z. H.; Ostermann, J. M.; Enchelmaier, R.; Spatz, J. P.; Moller, M. *J. Am. Chem. Soc.* **2001**, *123*3147–3148.
(17) Park, M.; Harrison, C.; Chaikin, P. M.; Register, R. A.; Adamson, D. H. *Science* **1997**, *276*, 1401–1404.
(18) Thurn-Albrecht, T.; Schotter, J.; Kastle, C. A.; Emley, N.; Shibauchi, T.; Krusin-Elbaum, L.; Guarini, K.; Black, C. T.; Tuominen, M. T.; Russell, T. P. *Science* **2000**, *290*, 2126–2129.
(19) Li, Z.; Zhao, W.; Liu, Y.; Rafailovich, M. H.; Sokolov, J.; Khougaz, K.; Eisenberg, A.; Lennox, R. B.; Krausch, G. *J. Am. Chem. Soc.* **1996**, *118*, 10892–10893.
(20) Silva, G. A.; Czeisler, C.; Niece, K. L.; Beniash, E.; Harrington, D. A.; Kessler, J. A.; Stupp, S. I. *Science* **2004**, *303*, 1352–1355.
(21) Stupp, S. I. *MRS Bull.* **2005**, *30*, 546–553.
(22) Vriezema, D. M.; Aragones, M. C.; Elemans, J.; Cornelissen, J.; Rowan, A. E.; Nolte, R. J. M. *Chem. Rev.* **2005**, *105*, 1445–1489.
(23) Kataoka, K.; Harada, A.; Nagasaki, Y. *Adv. Drug Delivery Rev.* **2001**, *47*, 113–131.
(24) Fustin, C. A.; Abetz, V.; Gohy, J. F. *Eur. Phys. J. E* **2005**, *16*, 291–302.
(25) Zhong, S.; Cui, H. G.; Chen, Z. Y.; Wooley, K. L.; Pochan, D. J. *Soft Matter* **2008**, *4*, 90–93.
(26) Zhu, J. T.; Jiang, W. *Macromolecules* **2005**, *38*, 9315–9323.
(27) Li, Z. B.; Hillmyer, M. A.; Lodge, T. P. *Langmuir* **2006**, *22*, 9409–9417.
(28) Li, Z. B.; Hillmyer, M. A.; Lodge, T. P. *Nano Lett.* **2006**, *6*, 1245–1249.
(29) Stewart, S.; Liu, G. J. *Chem. Mater.* **1999**, *11*, 1048–1054.
(30) Kriz, J.; Masar, B.; Plestil, J.; Tuzar, Z.; Pospisil, H.; Doskocilova, D. *Macromolecules* **1998**, *31*, 41–51.
(31) Yu, G. E.; Eisenberg, A. *Macromolecules* **1998**, *31*, 5546–5549.
(32) Ishizone, T.; Sugiyama, K.; Sakano, Y.; Mori, H.; Hirao, A.; Nakahama, S. *Polym. J.* **1999**, *31*, 983–988.
(33) Talingting, M. R.; Munk, P.; Webber, S. E.; Tuzar, Z. *Macromolecules* **1999**, *32*, 1593–1601.
(34) Stewart, S.; Liu, G. *Angew. Chem., Int. Ed.* **2000**, *39*, 340–344.
(35) Yan, X. H.; Liu, G. J.; Li, Z. *J. Am. Chem. Soc.* **2004**, *126*, 10059–10066.
(36) Lei, L. C.; Gohy, J. F.; Willet, N.; Zhang, J. X.; Varshney, S.; Jerome, R. *Macromolecules* **2004**, *37*, 1089–1094.
(37) Guo, A.; Liu, G. J.; Tao, J. *Macromolecules* **1996**, *29*, 2487–2493.
(38) Liu, G. J.; Qiao, L. J.; Guo, A. *Macromolecules* **1996**, *29*, 5508–5510.
(39) Cornelissen, J.; Fischer, M.; Sommerdijk, N.; Nolte, R. J. M. *Science* **1998**, *280*, 1427–1430.
(40) Geng, Y.; Discher, D. E.; Justynska, J.; Schlaad, H. *Angew. Chem., Int. Ed.* **2006**, *45*, 7578–7581.
(41) Krappe, U.; Stadler, R.; Voigtmartin, I. *Macromolecules* **1995**, *28*, 4558–4561.
(42) Xiang, H.; Shin, K.; Kim, T.; Moon, S. I.; McCarthy, T. J.; Russell, T. P. *Macromolecules* **2005**, *38*, 1055–1056.
(43) Bates, F. S.; Fredrickson, G. H. *Phys. Today* **1999**, *52*, 32–38.
(44) Narasimhan, V.; Huang, R. Y. M.; Burns, C. M. *J. Polym. Sci. B: Polym. Phys.* **1983**, *21*, 1993–2001.
(45) Zheng, R. H.; Liu, G. J.; Yan, X. H. *J. Am. Chem. Soc.* **2005**, *127*, 15358–15359.
(46) Gohy, J. F.; Khousakoun, E.; Willet, N.; Varshney, S. K.; Jerome, R. *Macromol. Rapid Commun.* **2004**, *25*, 1536–1539.
(47) Hu, J. W.; Liu, G. J. *Macromolecules* **2005**, *38*, 8058–8065.
(48) Li, J. X.; Ness, J. N.; Cheung, W. L. *J. Appl. Polym. Sci.* **1996**, *59*, 1733–1740.
(49) Yan, X. H.; Liu, G. J.; Haeussler, M.; Tang, B. Z. *Chem. Mater.* **2005**, *17*, 6053–6059.
(50) Liu, G. J.; Lu, Z. H.; Duncan, S. *Macromolecules* **2004**, *37*, 4218–4226.
(51) Njikang, G.; Liu, G.; Gao, J. *Macromolecules* **2007**, *40*, 9174–9180.
(52) Liu, G. J.; Ding, J. F.; Qiao, L. J.; Guo, A.; Dymov, B. P.; Gleeson, J. T.; Hashimoto, T.; Saijo, K. *Chem. Eur. J.* **1999**, *5*, 2740–2749.
(53) Brandrup, J.; Immergut, E. H. *Polymer Handbook*, 3rd ed.; John Wiley & Sons: New York, 1989.
(54) Yan, X. H.; Liu, G. J.; Liu, F. T.; Tang, B. Z.; Peng, H.; Pakhomov, A. B.; Wong, C. Y. *Angew. Chem., Int. Ed.* **2001**, *40*, 3593–3596.
(55) Elias, H.-G. *An Introduction to Polymer Science*; VCH Publishers: Weinheim, 1997.
(56) Battaglia, G.; Ryan, A. J. *J. Am. Chem. Soc.* **2005**, *127*, 8757–8764.
(57) Forster, S.; Zisenis, M.; Wenz, E.; Antonietti, M. *J. Chem. Phys.* **1996**, *104*, 9956–9970.
(58) Jain, S.; Bates, F. S. *Macromolecules* **2004**, *37*, 1511–1523.
(59) Zhang, Z. R.; Liu, G. J.; Bell, S. *Macromolecules* **2000**, *33*, 7877–7883.
(60) van Krevelen, D. W. *Properties of Polymers—Their Correlation with Chemical Structure; Their Numerical Estimation and Prediction from Additive Group Contributions*, 3rd ed.; Elsevier Science: Amsterdam, 1997.
(61) Lin, K. C.; Weis, R. M.; McConnell, H. M. *Nature* **1982**, *296*, 164–165.
(62) Huang, J. R. *Eur. Phys. J. E* **2006**, *19*, 399–412.

MA801626Y